

Multi-Person Pose Estimation Evaluation Using Optimal Transportation and Improved Pose Matching

Takato Moriki Hiromu Taketsugu Norimichi Ukita
Toyota Technological Institute
{25440,25502,ukita}@toyota-ti.ac.jp

Abstract

In Multi-Person Pose Estimation (MPPE), many metrics place importance on ranking of pose detection confidence scores. Current metrics tend to disregard false-positive poses with low confidence, focusing primarily on a larger number of high-confidence poses. Consequently, these metrics may yield high scores even when many false-positive poses with low confidence are detected. For fair evaluation taking into account a tradeoff between true-positive and false-positive poses, this paper proposes Optimal Correction Cost for pose (OCpose), which evaluates detected poses against pose annotations as an optimal transportation. For the fair tradeoff between true-positive and false-positive poses, OCpose equally evaluates all the detected poses regardless of their confidence scores. In OCpose, on the other hand, the confidence score of each pose is utilized to improve the reliability of matching scores between the estimated pose and pose annotations. As a result, OCpose provides a different perspective assessment than other confidence ranking-based metrics.

1 Introduction

Multi-person pose estimation (MPPE) detects the keypoints of people in images as a set of 2D image coordinates [1–5]. MPPE is crucial in various applications [6–10]. MPPE is evaluated based on the rank of the confidence scores of the detected poses in major metrics, such as mAP [11], BBP [12], and others [13].

While these metrics are widely used in the literature, they have a critical issue in evaluating how each pose estimation method is useful in real applications. This issue is shown in Fig. 1, which shows the precision-recall curves drawn by different pose detection thresholds of the same pose estimation method. Each curve is drawn by calculating the precision score (i.e., the vertical axis) of detected poses selected in descending order of the detection confidence score. The curve moves to the right as the recall score is incremented along the horizontal axis. Since many poses are detected with high confidence scores thanks to recent object detection and human pose estimation methods, this curve is almost saturated until the recall score gets larger. Therefore, in general, the difference between the curves appears after they begin to decline. Each curve vertically drops to 0 when all detected poses are evaluated.

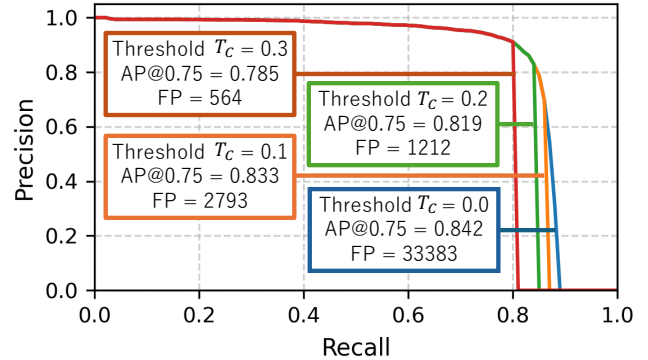


Figure 1. Unfair evaluation in mAP, which is a major evaluation metric using the confidence rank. Lower thresholds lead to high scores (AP) while producing many false-positives (FP).

As shown in Fig. 1, the curves drop in descending order of the confidence threshold (i.e., $T_c = 0.3, 0.2, 0.1,$ and 0.0 in Fig. 1). While the area under curve is regarded as the evaluation score (i.e., Average Precision, AP) of each pose estimation method, the scores of these different confidence thresholds are similar because the left area covered by the almost saturated precision scores is dominant. What is worse is that the evaluation score gradually increases by lowering the confidence threshold even after the curve begins to decline, while the lower threshold produces a large number of false-positive poses. For example, in Fig. 1, while the AP score increases from 0.785 ($T_c = 0.3$) to 0.842 ($T_c = 0.0$), the number of false positives significantly increases from 564 ($T_c = 0.3$) to 33,383 ($T_c = 0.0$).

To address the problem of the confidence ranking-based metrics, this paper proposes Optimal Correction Cost for pose (OCpose) with the contributions below:

- **Evaluation metric without confidence ranking:** OCpose uses optimal transportation (OT) to equally penalize false-positive poses [14–18].
- **Confidence-based pose matching:** Matching scores between estimated poses and pose annotations are improved with the confidence scores of pose keypoints.
- **User evaluation:** OCpose aligns better with human preferences than other metrics; see Fig. 2.

	1	2	...	N	mAP (\uparrow)	OCpose (\downarrow)
Estimator A			...		0.776 Best	0.778
Estimator B			...		0.754	0.298 Best

Figure 2. Difference between mAP and OCpose. Red circles highlight false positives. mAP favors Estimator A despite many false positives, whereas OCpose prioritizes Estimator B with fewer false detections.

	GT poses	...	GT masks	...	GT crowd masks	Dummy GT
Estimated Poses			$C_{d,g}$
	$C_{1,1}$...	$C_{1,j}$...	$C_{1,n}$	$C_{d,g}$
	\vdots	\vdots	\vdots	\vdots	\vdots	\vdots
			$C_{d,g}$
	$C_{m,1}$...	$C_{m,j}$...	$C_{m,n}$	$C_{d,g}$
Dummy esti	$C_{d,e}$...	$C_{d,e}$...	$C_{d,e}$	0

(1)OKS_p (2)OKS_m (3)OKS_c

Figure 3. Overview of OCpose. Given GT poses, masks, crowd masks, and estimated poses, OT costs between them are calculated to determine the evaluation score.

2 Related Work

2.1 Multi-Person Pose Estimation Evaluation

In MPPE, pose similarity between each estimated pose and a Ground Truth (GT) annotation pose is used to evaluate the pose estimation score of the whole image. Note that this similarity differs from the pose detection confidence given by a pose estimation network; after each pose with its confidence is detected, the pose similarity between the detected pose and each GT pose is evaluated. For example, Object Keypoint Similarity [3] (OKS) is used as the pose-matching scores in mAP. OKS is calculated by the distance between the keypoints of an estimated pose and its nearest GT. If OKS exceeds a threshold, the estimated pose is considered a true positive; otherwise, it is a false positive.

However, a major issue in MPPE is that GT poses are unavailable for several people, such as tiny peo-

ple. To address this issue, other simpler annotations are provided. For example, in The Microsoft Common Objects in Context 2017 (COCO) [11], people without GT pose annotations are with either of “GT bounding box (bbox)” given to each person or “GT crowd bbox” given to a person crowd. As with the GT pose, these GT bbox and GT crowd bbox are used to calculate OKS of each estimated pose. In several metrics [12, 13], if OKS exceeds the threshold, this pose is excluded from the evaluation. Otherwise, this pose is regarded as a false positive. However, these metrics rely on confidence ranking, so they do not address the problem highlighted in Sec. 1.

2.2 Optimal Transportation Evaluation

OT computes a distance between probability distributions. In [15], OT is incorporated into the object detection task. OC-cost [14] uses OT as a metric for object detection. Since OT evaluates detection accuracy and overdetectability independently of the rank of detection confidences, our OCpose also employs OT.

3 Proposed Evaluation Metric for MPPE

OCpose calculates the score in two steps. The first step (Sec. 3.1) is to calculate the matching scores of all possible combinations between estimated poses and GT annotations (Fig. 3). The second step (Sec. 3.2) is the combinatorial optimization of the matching scores.

3.1 Pose Matching

In OCpose, the following three matching scores (OKS_p, OKS_m, and OKS_c) are used.

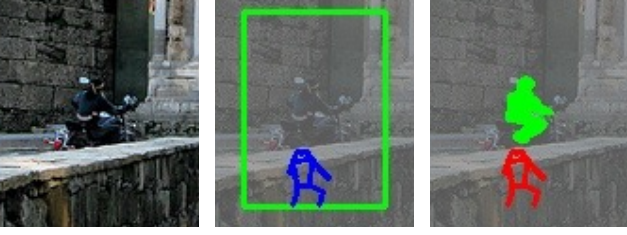
Matching with GT poses. OKS_p, which is the matching score between an estimated pose and a GT pose (shown in Fig. 3 (1)), is defined by the 2D keypoint coordinates of these two poses [11]; as the distance between the keypoints of these two poses gets smaller, OKS_p becomes larger. The reliability of OKS_p is improved by the visibility of each GT keypoint, which is available as the annotation, so that invisible keypoints are not used. OCpose uses OKS_p as is.

Matching with GT masks. In the literature, OKS_m, originally proposed for evaluating object detections, is reused as the matching score between an estimated pose and a GT bbox as follows:

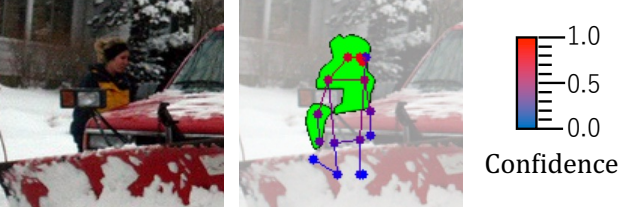
$$\text{OKS}_b = \frac{1}{N} \sum_{n=1}^N \exp\left(-\frac{(d_b(x_d^n, y_d^n, b))^2}{2s^2k_n^2}\right) \quad (1)$$

$$d_b(x_d^n, y_d^n, b) = \min(x_d^n, y_d^n, b) \quad (2)$$

where $\min(x_d^n, y_d^n, b)$ is the minimum distance from the estimated keypoint (x_d^n, y_d^n) to its nearest boundary of the GT bbox b . Since the bbox is larger than the set of GT keypoints, Eq. (1) over-accepts the detected poses



(a) image (b) bbox (c) mask
 Figure 4. Comparison of bbox and mask annotations, which are indicated by green rectangles in (b) and green pixels in (c), respectively. While the bbox incorrectly accepts the false pose colored blue in (b), the mask can recognize it as a false positive in (c).



(a) image (b) keypoints
 Figure 5. Confidence-based pose matching. Although several keypoints are located outside the mask, their low confidence reduces the influence on the OKS. In contrast, conventional OKS may penalize such poses regardless of confidence.

as true positives. While Eq. (1) uses the GT bbox because the prediction output of object detection is a bbox, our matching function should be optimized for human keypoints. Thus, OCpose replaces a GT bbox in Eq. (1) with a pixel-wise mask denoted by m :

$$\text{OKS}_m = \frac{1}{N} \sum_{n=1}^N \exp \left(-\frac{(d_m(x_d^n, y_d^n, c_d^n, m))^2}{2s^2k_n^2} \right) \quad (3)$$

$$d_m(x_d^n, y_d^n, c_d^n, m) = \min(x_d^n, y_d^n, m) \times \frac{c_d^n}{\sum_{n=1}^N c_d^n}, \quad (4)$$

where $\min(x_d^n, y_d^n, m)$ is the minimum distance from (x_d^n, y_d^n) to its nearest pixel on the mask. c_d^n denotes the confidence score of the n -th keypoint of a detected person. c_d^n encourages OKS_m to be larger with keypoints with higher confidence, each of which is expected to be visible inside the mask (Fig. 5). Therefore, OKS_m can avoid the incorrect over-acceptance of true positives.

Matching with GT crowd masks OKS_c is the matching score between an estimated pose and a GT crowd mask (shown in Fig. 3 (3)). The definition and motivation of OKS_c are the same as those of OKS_m . That is, to suppress false positives detected due to a large number of non-human pixels in a crowd bbox, OCpose uses pixel-wise crowd masks.

3.2 Combinatorial Optimization

In Eq. (5), the matching scores (OKS_p , OKS_m , OKS_c) are used to compute the OT costs $C_{i,j}$ stored in a table, which is called the cost matrix shown in Fig. 3.

$$C(i, j) = 1 - \text{OKS}(d_i, g_j), \quad (5)$$

where $\text{OKS}(d_i, g_j)$ is OKS between the i -th estimated pose d_i and the j -th GT annotation g_j , including GT poses, GT bboxes, and GT crowd bboxes. The range of $C(i, j)$ is $0 \leq C(i, j) \leq 1$. While OC-cost [14] for object detection evaluation has only GT bboxes, corresponding to GT poses for MPPE evaluation, our OCpose has GT masks and GT crowd masks as well.

OT optimizes the combination between the estimated poses and the GT annotation so that each estimated pose matches with one of the GT annotation by minimizing the following function:

$$\text{OC}_{\text{pose}} = \frac{1}{|\Pi_1|} \sum_{i=1}^{N_g} \sum_{j=1}^{N_e} C(i, j) \cdot \pi_{i,j}, \quad (6)$$

where N_e and N_g denote the numbers of the estimated poses and the GT annotation, respectively. In Eq. (6), $\pi_{i,j} \in \{0, 1\}$ is optimized. If $\pi_{i,j} = 1$, the i -th estimated pose matches with the j -th GT annotation. Π_1 is defined so that $\pi_{i,j}$ is included in Π_1 , if $\pi_{i,j} = 1$. While each of the GT poses and the GT masks matches with only one estimated pose, each GT crowd mask can match with multiple estimated poses. This is the difference from OC-cost [14] because OC-cost has no GT crowd masks. On the other hand, similar to OC-cost, our OCpose also implements dummy GTs to match over-detections when $N_e > N_g$, which imposes the costs. Also, when $N_e < N_g$, dummy estimated poses are used to impose costs. OCpose sets these costs to 1.

4 Experiments

4.1 Datasets

We evaluate OCpose using two standard benchmarks for MPPE. The first one is COCO [11], which provides annotations for both MPPE and instance segmentation masks. Another one is CrowdPose Dataset [19], which is specifically designed to evaluate MPPE in crowded scenes. Since CrowdPose Dataset does not provide mask annotation, we generated pseudo masks by state-of-the-art segmentation models [20, 21] using the provided GT bboxes.

4.2 Quantitative Results

We evaluate state-of-the-art MPPE methods [22–26], using both their default confidence thresholds and new thresholds optimized to minimize the OCpose

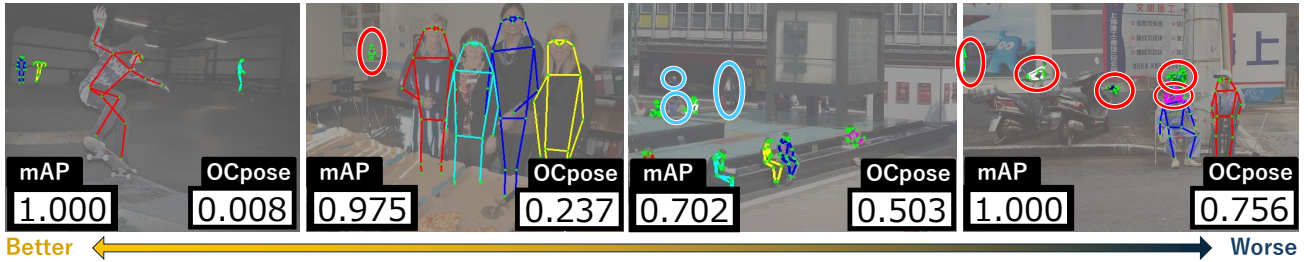


Figure 6. Example of OCpose. The score is descending from left to right. The leftmost image succeeds in accurate MPPE. Other images have missing poses (blue circles) or false positives (red circles).

Table 1. Comparison of evaluations in COCO. “threshold” indicates confidence thresholds where “-” represents the one optimized by the authors of each paper and “o” represents the one minimizing OCpose.

	threshold	mAP(↑)	OC pose(↓)
BUCTD [22]	- (0.00)	0.776	0.778
	o (0.16)	0.761	0.292
RTMO [23]	- (0.10)	0.724	0.621
	o (0.45)	0.706	0.381
CID [24]	- (0.01)	0.694	0.537
	o (0.04)	0.668	0.403
ViTPose [25]	- (0.00)	0.768	0.792
	o (0.41)	0.748	0.285
HRNet [26]	- (0.00)	0.763	0.802
	o (0.34)	0.748	0.288

Table 2. Comparison of evaluations in CrowdPose. ViTPose and HRNet are not shown because human pose detections are not officially available.

	threshold	mAP(↑)	OCpose(↓)
BUCTD [22]	- (0.00)	0.785	0.891
	o (0.18)	0.744	0.239
RTMO [23]	- (0.10)	0.839	0.412
	o (0.46)	0.824	0.188
CID [24]	- (0.01)	0.712	0.308
	o (0.02)	0.703	0.255

score (Tables 1, 2). We show that optimizing for OCpose leaves mAP nearly unchanged while significantly reducing the OCpose score, and that optimal thresholds vary substantially across models. This optimizing is demonstrated in Sec. 4.3, 4.4.

4.3 Qualitative Results

Examples of OCpose (Fig. 6) show that OCpose becomes lower (i.e., better) if only true-positive poses are detected, as shown in the leftmost example. We can see that OCpose appropriately penalizes not only false-negatives (i.e., blue circles in Fig. 6) but also false-positives (i.e., red circles in Fig. 6).

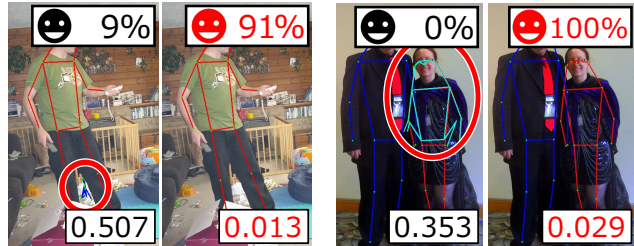


Figure 7. Example images of subjective evaluations. In each image pair, the left one is the result with the default threshold, and the right one is the result with the threshold optimized by OCpose. The percentage next to the smile button represents the user preference. The OCpose scores are in the lower right corner. Red circles indicate false positives. The trends of OCpose and the user preference are consistent.

4.4 Agreement with Human Preference

In our subjective evaluation with 36 participants, human poses detected by CID [24] with its default confidence threshold are compared with those detected by the OCpose-optimized threshold. Subjects selected the better one from these two poses detected in 100 randomly selected COCO images (Fig. 7). The results of the OCpose-optimized threshold were selected with **83.3** percent of the evaluations.

5 Conclusion

This paper proposes OCpose, a novel evaluation metric for MPPE that addresses the problems of mAP. By the optimal transportation with improved cost calculation, OCpose appropriately evaluates false-positive poses, which mAP tends to neglect. Our OCpose suggests the benefit of having a different perspective from other evaluation metrics, such as mAP. We believe this contribution provides a more thorough evaluation framework for MPPE methods and serves as a valuable toolkit for both researchers and downstream application developers.

References

- [1] Haoming Chen, Runyang Feng, Sifan Wu, Hao Xu, Fengcheng Zhou, and Zhenguang Liu. 2d human pose estimation: a survey. *Multim. Syst.*, 29(5):3115–3138, 2023.
- [2] Gongjin Lan, Yu Wu, Fei Hu, and Qi Hao. Vision-based human pose estimation via deep learning: A survey. *IEEE Trans. Hum. Mach. Syst.*, 53(1):253–268, 2023.
- [3] T.-Y. Lin, G. Patterson, M. R. Ronchi, Y. Cui, M. Maire, S. Belongie, L. Bourdev, R. Girshick, J. Hays, P. Perona, D. Ramanan, L. Zitnick, and P. Dollár. Coco keypoints challenge, 2016. <https://cocodataset.org/#keypoints-eval>.
- [4] Mykhaylo Andriluka, Leonid Pishchulin, Peter V. Gehler, and Bernt Schiele. 2d human pose estimation: New benchmark and state of the art analysis. In *CVPR*, pages 3686–3693, 2014.
- [5] Marcin Eichner and Vittorio Ferrari. We are family: Joint pose estimation of multiple persons. In *ECCV*, pages 228–242, 2010.
- [6] Henry M. Clever, Zackory Erickson, Ariel Kapusta, Greg Turk, C. Karen Liu, and Charles C. Kemp. Bodies at rest: 3d human pose and shape estimation from a pressure image using synthetic data. In *CVPR*, pages 6214–6223, 2020.
- [7] Tobias Baumgartner and Stefanie Klatt. Monocular 3d human pose estimation for sports broadcasts using partial sports field registration. In *CVPRW*, pages 5109–5118, 2023.
- [8] Mickael Cormier, Aris Clepe, Andreas Specker, and Jürgen Beyerer. Where are we with human pose estimation in real-world surveillance? In *WACVW*, pages 591–601. IEEE, 2022.
- [9] R. James Cotton. Posepipe: Open-source human pose estimation pipeline for rehabilitation research. *Archives of Physical Medicine and Rehabilitation*, 103(12):e161–e162, 2022.
- [10] Manolis Vasileiadis, Sotiris Malassiotis, Dimitrios Giakoumis, Christos-Savvas Bouganis, and Dimitrios Tzovaras. Robust human pose tracking for realistic service robot applications. In *ICCVW*, pages 1363–1372, 2017.
- [11] Tsung-Yi Lin, Michael Maire, Serge J. Belongie, James Hays, Pietro Perona, Deva Ramanan, Piotr Dollár, and C. Lawrence Zitnick. Microsoft COCO: common objects in context. In *ECCV*, pages 740–755, 2014.
- [12] Yu Cheng, Yihao Ai, Bo Wang, Xinchao Wang, and Robby T. Tan. Bottom-up 2d pose estimation via dual anatomical centers for small-scale persons. *Pattern Recognit.*, 139:109403, 2023.
- [13] Mykhaylo Andriluka, Umar Iqbal, Eldar Insafutdinov, Leonid Pishchulin, Anton Milan, Juergen Gall, and Bernt Schiele. Posetrack: A benchmark for human pose estimation and tracking. In *CVPR*, 2018.
- [14] Mayu Otani, Riku Togashi, Yuta Nakashima, Esa Rahtu, Janne Heikkilä, and Shin’ichi Satoh. Optimal correction cost for object detection evaluation. In *CVPR*, pages 21075–21083, 2022.
- [15] Zheng Ge, Songtao Liu, Zeming Li, Osamu Yoshie, and Jian Sun. OTA: optimal transport assignment for object detection. In *CVPR*, pages 303–312, 2021.
- [16] Cong Yu, Dongheng Zhang, Zhi Wu, Zhi Lu, Chunyang Xie, Yang Hu, and Yan Chen. Rfpose-ot: Rf-based 3d human pose estimation via optimal transport theory. *Frontiers Inf. Technol. Electron. Eng.*, 24(10):1445–1457, 2023.
- [17] Lu Zhou, Yingying Chen, Yunze Gao, Jinqiao Wang, and Hanqing Lu. Occlusion-aware siamese network for human pose estimation. In *ECCV*, pages 396–412, 2020.
- [18] Xiang Gu, Yucheng Yang, Wei Zeng, Jian Sun, and Zongben Xu. Keypoint-guided optimal transport with applications in heterogeneous domain adaptation. In *NeurIPS*, 2022.
- [19] Jiefeng Li, Can Wang, Hao Zhu, Yihuan Mao, Haoshu Fang, and Cewu Lu. Crowdpose: Efficient crowded scenes pose estimation and a new benchmark. In *CVPR*, 2019.
- [20] Alexander Kirillov, Eric Mintun, Nikhila Ravi, Hanzi Mao, Chloé Rolland, Laura Gustafson, Tete Xiao, Spencer Whitehead, Alexander C. Berg, Wan-Yen Lo, Piotr Dollár, and Ross B. Girshick. Segment anything. In *ICCV*, pages 3992–4003, 2023.
- [21] Maxime Oquab, Timothée Darcet, Théo Moutakanni, Huy V. Vo, Marc Szafranec, Vasil Khalidov, Pierre Fernandez, Daniel Haziza, Francisco Massa, Alaaeldin El-Nouby, Mido Assran, Nicolas Ballas, Wojciech Galuba, Russell Howes, Po-Yao Huang, Shang-Wen Li, Ishan Misra, Michael Rabbat, Vasu Sharma, Gabriel Synnaeve, Hu Xu, Hervé Jégou, Julien Mairal, Patrick Labatut, Armand Joulin, and Piotr Bojanowski. DINOv2: Learning robust visual features without supervision. *Trans. Mach. Learn. Res.*, 2024, 2024.
- [22] Mu Zhou, Lucas Stofl, Mackenzie Weygandt Mathis, and Alexander Mathis. Rethinking pose estimation in crowds: overcoming the detection information bottleneck and ambiguity. In *ICCV*, 2023.
- [23] Peng Lu, Tao Jiang, Yining Li, Xiangtai Li, Kai Chen, and Wenming Yang. RTMO: towards high-performance one-stage real-time multi-person pose estimation. In *CVPR*, 2024.
- [24] Dongkai Wang and Shiliang Zhang. Contextual instance decoupling for robust multi-person pose estimation. In *CVPR*, 2022.
- [25] Yufei Xu, Jing Zhang, Qiming Zhang, and Dacheng Tao. Vitpose: Simple vision transformer baselines for human pose estimation. In *NeurIPS*, 2022.
- [26] Jingdong Wang, Ke Sun, Tianheng Cheng, Borui Jiang, Chaorui Deng, Yang Zhao, Dong Liu, Yadong Mu, Mingkui Tan, Xinggang Wang, Wenyu Liu, and Bin Xiao. Deep high-resolution representation learning for visual recognition. *IEEE Trans. Pattern Anal. Mach. Intell.*, 2021.